

# Thermodynamic Studies on the Interaction of Antibodies with $\beta$ -Amyloid Peptide

Manfred Brockhaus,<sup>§</sup> Peter Ganz,<sup>†</sup> Walter Huber,<sup>§</sup> Bernd Bohrmann,<sup>§</sup>  
Hans-Ruedi Loetscher,<sup>§</sup> and Joachim Seelig<sup>\*,†</sup>

Department PRBD, F. Hoffmann-La Roche Ltd., CH-4070 Basel, Switzerland, and Department of Biophysical Chemistry, Biozentrum, University of Basel, Klingelbergstrasse 50/70, CH-4056 Basel, Switzerland

Received: September 29, 2006; In Final Form: November 28, 2006

Antibodies against  $\beta$ -amyloid peptides ( $A\beta$ s) are considered an important therapeutic opportunity in Alzheimer's disease. Despite the vast interest in  $A\beta$  no thermodynamic data on the interaction of antibodies with  $A\beta$  are available as yet. In the present study we use isothermal titration calorimetry (ITC) and surface plasmon resonance to provide a quantitative thermodynamic analysis of the interaction between soluble monomeric  $A\beta$ (1–40) and mouse monoclonal antibodies (mAb). Using four different antibodies directed against the N-terminal, middle, and C-terminal  $A\beta$  epitopes, we measured the thermodynamic parameters for the binding to  $A\beta$ . Each antibody species was found to have two independent and equal binding sites for  $A\beta$  with binding constants in the range of  $10^7$  to  $10^8$  M<sup>-1</sup>. The binding reaction was essentially enthalpy driven with a reaction enthalpy of  $\Delta H_{A\beta}^0 \approx -19$  to  $-8$  kcal/mol, indicating the formation of tight complexes. The loss in conformational freedom was supported by negative values for the reaction entropy  $\Delta S_{A\beta}^0$ . We also measured the heat capacity change of the 1mAb:2 $A\beta$  reaction.  $\Delta C_{p,A\beta}^0$  was large and negative but could not be explained exclusively by the hydrophobic effect. The free energy of binding was found to be linearly correlated with the size of the epitope.

The presence of amyloid containing plaques in the brain of Alzheimer's disease patients is one major neuropathological hallmark of the disease. The plaques which contain the 40 or 42 amino acid long peptide  $A\beta$  are the focus of intense research efforts for developing Alzheimer's disease therapeutics. Antibodies against  $A\beta$  have been found to be highly efficient in removing  $A\beta$  and diffuse plaques from the brains of transgenic mice which serve as an animal model for Alzheimer's disease.<sup>1</sup> A clinical trial of active vaccination in Alzheimer's disease patients has shown a similar efficacy of  $A\beta$  specific antibodies in reducing  $A\beta$  deposits in the human brain.<sup>2</sup> Hence, active or passive vaccination with anti- $A\beta$ -antibodies is considered by many as the most promising route toward treating Alzheimer's disease.

Antibodies differ widely in terms of antigen recognition and affinity. For anti- $A\beta$ -antibodies an N-terminal epitope recognition together with a high affinity for  $A\beta$  appear to be of paramount importance for efficacy in treating the brain symptoms in transgenic mouse models of Alzheimer's disease.<sup>3,4</sup> However, an antibody directed against the middle part of  $A\beta$  has also been described as being efficacious.<sup>5</sup> Despite the strong medical interest in anti- $A\beta$ -antibodies nothing is known about the thermodynamic parameters which govern the equilibrium reaction between  $A\beta$  free in solution and antibody-bound  $A\beta$ . Since  $A\beta$  has the tendency to aggregate and to precipitate as highly structured fibrils the interaction with antibody will also depend on the aggregation status of  $A\beta$ . The interaction of antibodies with  $A\beta$  may alter the aggregation properties of  $A\beta$  and the tendency to form oligomers and highly structured fibrils.

It should also be realized that lipid membranes may play an important part in the  $A\beta$  aggregation process.  $A\beta$  peptide can either be firmly anchored in a membrane, thereby preventing release and aggregation, or it can undergo enhanced aggregation at the surface of a negatively charged membrane.<sup>6–8</sup>

Here we use isothermal calorimetry (ITC) with soluble  $A\beta$ -(1–40) and a set of four anti- $A\beta$  monoclonal antibodies to measure the enthalpy and entropy changes that govern the antibody binding to  $A\beta$ . The antibody affinities are also measured by surface plasmon resonance and compared to the equilibrium constants obtained by ITC. In addition, we discuss the potential influence of different epitope specificities for the observed entropy changes. We show that the temperature dependence of the antibody binding indicates that hydrophobic as well as polar interactions contribute to the binding process.

## Experimental Procedures

**Peptides and Antibodies.**  $A\beta$ (1–40) was either obtained from a commercial source (Bachem, Bubendorf, Switzerland) or prepared by the in-house peptide facility. A critical property of  $A\beta$  peptides is the transition from their soluble form, which is mainly random coil, to a  $\beta$ -structured aggregate. This process has been studied with synthetic  $A\beta$ s where the replacement of amino acids by their D-enantiomers induces a destabilization of the secondary structure without changing other properties of the peptide.<sup>9</sup> As a control for antibody B1-N which detects a minimum epitope comprising amino acids 4–6 of  $\beta A$ (1–40) we have employed the peptide D,D5,6 $A\beta$ (1–40). It contains D-amino acids at positions 5 and 6. D,D5,6 $A\beta$ (1–40) was a generous gift of Dr. M. Beyermann, Forschungsinstitut Molekulare Pharmakologie, Berlin–Buch.

**Antibodies.** The four monoclonal antibodies are derived from three different mouse immunizations; the B-number refers to a

\* Address correspondence this author. Phone: +41-61-267 2190. Fax: +41-61-267 2189. E-mail: joachim.seelig@unibas.ch.

<sup>§</sup> F. Hoffmann-La Roche Ltd.

<sup>†</sup> University of Basel.

**TABLE 1: Thermodynamic Parameters for the Binding of Alzheimer Peptide A $\beta$ (1–40) to Different Antibodies As Deduced with Isothermal Titration Calorimetry (ITC) and Surface Plasmon Resonance (SPR)<sup>a</sup>**

antibody	minimum epitope	binding constant $K_0$ , <sup>a</sup> M <sup>-1</sup>	$K_{\text{diss,ITC}}$ , nM	$\Delta H_{\text{A}\beta}^0$ , <sup>a</sup> kcal/mol	$\Delta G_{\text{A}\beta}^0$ , kcal/mol	$T\Delta S_{\text{A}\beta}^0$ , kcal/mol	$\Delta S_{\text{A}\beta}^0$ , cal/(mol K)	$C_{p,\text{A}\beta}^0$ , cal/(mol K)	$K_{\text{diss,SPR}}$ , <sup>b</sup> nM
B1-N	4–6 FRH	$3.5 \times 10^7$	29	–17.6	–10.4	–7.3	–24.1	$-214 \pm 100$	43
B24-C40	35–39 MVGGV	$5.1 \times 10^7$	20	–8.1	–10.6	+2.4	8.1	$-363 \pm 20$	6
B41-N	5–10 RHDSGY	$7.2 \times 10^7$	14	–17.1	–10.8	–6.3	–21.0	$-149 \pm 60$	85
B44-M	20–21 FA	$1.6 \times 10^7$	63	–19.4	–9.9	–10.4	–31.5	$-196 \pm 20$	41

<sup>a</sup> We estimate the error in evaluating  $\Delta H_{\text{A}\beta}^0$  as  $\pm 0.8$  kcal/mol. The main source of error is uncertainties arising from the peptide and antibody concentrations. The error in  $K_0$  for two identical measurements was typically about 30%. Figure 3 shows a comparison between measured and calculated  $K_0$  values, indicating only small deviations from the theoretical line. Similar good agreement was also obtained for the temperature dependence of the three other antibodies. All ITC measurements were made in 25 mM HEPES buffer at pH 7.4 and 28 °C. <sup>b</sup> SPR measurements: see Materials and Methods section.

chronological order, whereas the last letter indicates the specificity for the N-terminal (N), middle (M), or C-terminal A $\beta$  (C40) epitope (cf. Table 1). Antibody B1-N is an IgG2b derived from a mouse immunized with A $\beta$ (1–42). B24-C40 is an IgG-1 derived from an immunization with A $\beta$ (35–40) peptide-KLH conjugate. B41-N and B44-M are IgG1 antibodies derived from an immunization with A $\beta$ (1–28) cross-linked to KLH with glutaraldehyde. The antibodies were purified from hybridoma culture medium by hydrophobic interaction chromatography followed by anion exchange chromatography. The protein concentration was calculated from the optical density at 280 nm. All four antibodies are suited as specific reagents for sandwich immunoassays for A $\beta$  showing a sensitivity of 100 pg/mL. All calculations are based on a theoretical molecular weight for mouse IgG of 150 000 Da.

**Epitope Mapping.** Two independent methods were employed: (i) The first is an ELISA assay using hexapeptides from the A $\beta$  sequence coupled to BSA via a maleinimide linker. For this the hexapeptides were synthesized with an additional N-terminal or C-terminal cystein residue and reacted with *N*-hydroxysuccinimido-maleinimidopropionate (Pierce Biotechnology Inc., Rockford, IL) according to manufacturer's instructions. (ii) In the second assay the antibodies were reacted with immobilized decapeptides (pepspot, Jerini AG, Berlin, Germany) with subsequent immunoblotting and detection by enzyme chemoluminescence (ECL, Amersham-GE Healthcare, Piscataway, NJ). Both methods identify an epitope a few amino acids in length as it is contacted by an antibody against A $\beta$ .

**Isothermal Titration Calorimetry (ITC).** The solubility of A $\beta$ (1–40) depends on a variety of conditions such as temperature, salt concentration, pH, redox state of the peptide, and the experimental setup (adsorption phenomena). For oxidized and reduced A $\beta$  critical monomer concentrations in the range of 0.9–40  $\mu$ M have been reported, pertaining to different experimental situations.<sup>10–15</sup> ITC experiments<sup>16,17</sup> were performed with use of a Microcal VP-ITC calorimeter (Microcal, Northampton, MA) with Alzheimer peptide loaded into the cell at a concentration of typically 15–17  $\mu$ M. As the measurements were made at a low buffer concentration (25 mM HEPES, pH 7.4) and in the absence of salt, A $\beta$ (1–40) is not aggregated under these conditions.<sup>7</sup> The antibody solution was applied via an injection syringe at a concentration of  $\sim 10$ –12 mg/mL, corresponding to a molar concentration of 67–80  $\mu$ M. Both the titrant and the antibody were dissolved in the same buffer. Unless otherwise indicated, experiments were performed at 28 °C. In each experiment about 20–30 injections of 10  $\mu$ L of antibody solution were made into the cell containing the A $\beta$  peptide. The syringe stirring speed was set at 400 rpm. Control experiments were performed by injecting antibody into the dilution buffer. Only negligible heats of dilution were observed. The same was true by injecting pure buffer into the A $\beta$  peptide

solution. The experimental titration curves were corrected for heats of dilution and were fit to a multisite binding model (cf. below). The best fit curves yield the reaction enthalpy,  $\Delta H^0$ , and the association constant,  $K_0$ , as the thermodynamic parameters. The free energy,  $\Delta G^0$ , was calculated by using the relationship  $\Delta G^0 = -RT \ln K_0$ . The entropy,  $\Delta S^0$ , then followed from  $\Delta G^0 = \Delta H^0 - T\Delta S^0$ .

**Surface Plasmon Resonance (SPR).** SPR measurements were performed on a Biacore 3000 instrument (Biacore, Uppsala, Sweden) at 25 °C. HEPES buffer (10 mM HEPES, pH 7.4, 150 mM NaCl, 3 mM EDTA, 0.005% Tween 20) was used as the running buffer, as the immobilization buffer, and as the buffer to prepare the A $\beta$ (1–40) peptide and the antibody sample solutions. A CM5 sensor chip with a layer of carboxymethyl dextran was used for the binding experiments.

The A $\beta$ (1–40) was immobilized by standard amine coupling chemistry. The procedure included the activation of the carboxylic acid groups of the dextran layer during 7 min with a mixture of *N*-hydroxysuccinimide (NHS, 5.75 mg/mL) and 1-ethyl-3-(3-dimethylaminopropyl)carbodiimide (EDC, 32.5 mg/mL) and a contact of the activated surface with the peptide solution (20  $\mu$ M peptide in HEPES buffer) until the desired surface loading was obtained. The A $\beta$ (1–40) solutions were checked for the absence of oligomers and fibrils by analytical ultracentrifugation prior to immobilization. The amount of immobilized peptide corresponded to a sensor response of roughly 200 RU. The excess of activated carboxylic acid groups were quenched finally by contacting the surface for 5 min with a 1 M ethanolamine hydrochloride solution.

Binding experiments were performed by contacting the surface during 5 min with the antibody solution at a constant flow of 10  $\mu$ L/min. Binding experiments at 10 different concentrations were performed for the determination of one equilibrium binding constant. The equilibrium sensor responses monitored at the end of the injection phase were used to determine the equilibrium constants  $K_{\text{diss,SPR}}$  via a Scatchard analysis.

## Results

To characterize the antibody–A $\beta$  interaction in detail four different antibodies designated B1-N, B24-C40, B41-N, and B44-M were measured in the ITC experiment (cf. Table 1). As a typical titration, Figure 1 shows the reaction of a 14.2  $\mu$ M A $\beta$ (1–40) solution with 61.3  $\mu$ M B41-N (both in 25 mM HEPES, pH 7.4, 40 °C). The upper panel displays the heat flow as a function of consecutive 10  $\mu$ L B41-N antibody injections. During the initial phase of the titration the A $\beta$  peptide in the calorimeter cell ( $V_{\text{cell}} = 1.4037$  mL) is much in excess over the added antibody. A constant heat of reaction of  $h_i = -25$   $\mu$ cal is observed during the first few injections providing evidence

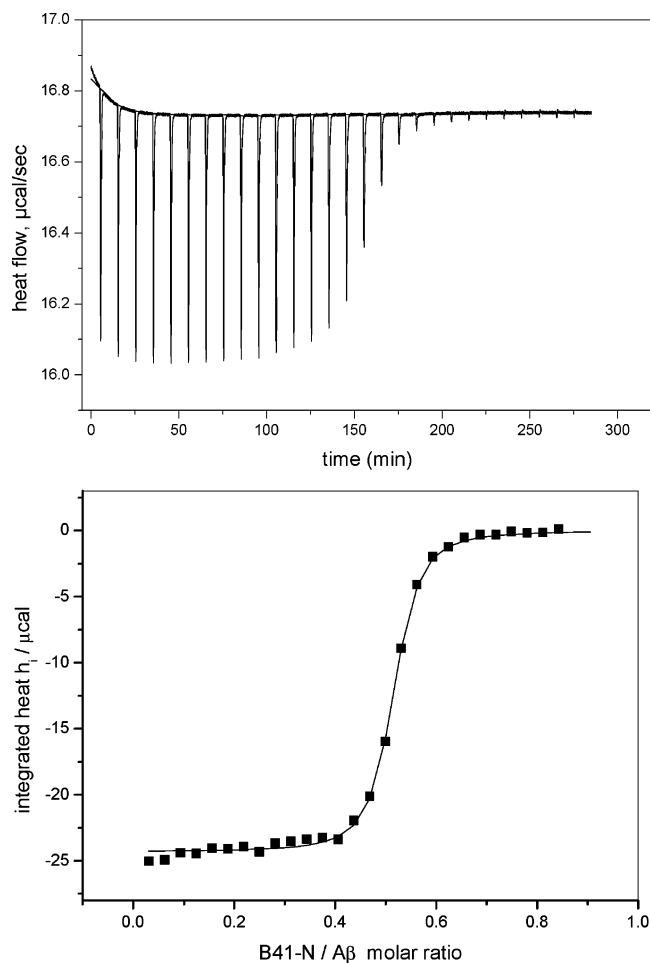


**Figure 1.** Titration of a 14.2  $\mu\text{M}$   $\text{A}\beta(1-40)$  solution in buffer (25 mM HEPES, pH 7.4) with a 61.3  $\mu\text{M}$  B41-N antibody solution in the same buffer. The injection of the antibody solution was in 10  $\mu\text{L}$  steps. The upper panel shows the heat flow,  $h_i$ , corrected for dilution effects, as a function of the B41-N/ $\text{A}\beta$  molar ratio. The lower panel displays the heats of injection,  $h_i$ , corrected for dilution effects, as a function of the B41-N/ $\text{A}\beta$  molar ratio. The solid line is the fit to a multisite binding model with  $\Delta H_{\text{A}\beta}^0 = -19.7$  kcal/mol,  $K_0 = 3 \times 10^7 \text{ M}^{-1}$ , and  $n = 2$  (2  $\text{A}\beta$  binding to 1 B41-N antibody). The measuring temperature was 40  $^\circ\text{C}$ .

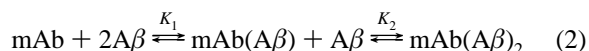
for a saturation of the antibody binding site(s) with  $\text{A}\beta$ . In Figure 1 the amount of antibody B41-N added per injection is 0.613 nmol, and the molar heat of antibody binding,  $\Delta H_{\text{mAb}}^0$ , is thus given by  $\Delta H_{\text{mAb}}^0 = -25/0.613 = -40.7$  kcal/mol. With increasing number of injections the  $\text{A}\beta$  in the calorimeter cell becomes complexed with antibody and no further heats of reaction are observed when the supply of free  $\text{A}\beta$  is exhausted. The small heat peaks at the last injections arise from dilution effects and are subtracted. The total heat of reaction is  $\sum h_i = -391$   $\mu\text{cal}$  and corresponds to the complexation of 19.7 nmol  $\text{A}\beta$ . The heat of reaction per mole of  $\text{A}\beta(1-40)$  is thus  $\Delta H_{\beta\text{AP}}^0 = -19.9$  kcal/mol. We can therefore conclude that each antibody molecule binds  $\Delta H_{\text{mAb}}^0/\Delta H_{\text{A}\beta}^0 = 2$  molecules  $\text{A}\beta$ . The ITC diagrams for the other antibodies investigated are qualitatively similar to Figure 1.

The lower panel in Figure 1 shows the integrated heats of reaction,  $h_i$ , corrected for dilution effects as a function of the B41-N/ $\text{A}\beta$  molar ratio. A quantitative analysis of the binding isotherm can be given by fitting the data to a multisite binding model:<sup>18</sup>

$$\frac{[\text{A}\beta]_{\text{bound}}}{[\text{mAb}]_{\text{total}}} = \frac{nK_0[\text{A}\beta]_{\text{free}}}{1 + K_0[\text{A}\beta]_{\text{free}}} \quad (1)$$

Here  $[\text{A}\beta]$  is the equilibrium concentration of  $\text{A}\beta$  (bound or free) and  $[\text{mAb}]_{\text{total}}$  is the total concentration of monoclonal antibody.  $n$  denotes the number of identical and independent binding sites on the antibody. The data fit to this model are given by the solid line in Figure 1 and yield the following parameters:  $n = 2$ ,  $\Delta H_{\text{A}\beta}^0 = -19.7$  kcal/mol,  $\Delta H_{\text{mAb}}^0 = 2\Delta H_{\text{A}\beta}^0 = -39.4$  kcal/mol, and  $K_0 = 3 \times 10^7 \text{ M}^{-1}$  (at 40  $^\circ\text{C}$ ). The analysis of the binding isotherm confirms the stoichiometry and the enthalpies derived from the initial and end values of the titration. In addition, it provides the binding constant  $K_0$  as a further parameter.

Considering the binding reaction in more detail we may write



The binding constants  $K_1$  and  $K_2$  are related to  $K_0$  according to  $K_1 = 2K_0$  and  $K_2 = 1/2K_0$ . The overall binding constant for the formation of  $\text{mAb}(\text{A}\beta)_2$  complex is  $K_T = K_1 \cdot K_2 = K_0^2$ . The binding constants  $K_1$  and  $K_2$  may be denoted as *macroscopic* binding constants while  $K_0$  is the *microscopic* binding constant.<sup>19</sup> In the following we will restrict the thermodynamic analysis to the microscopic constant  $K_0$ , which is the geometric average of  $K_1$  and  $K_2$ . The dissociation constant  $K_{\text{diss}}$  is then defined as  $K_{\text{diss}} = K_0^{-1}$ .

Our experiments demonstrate that the interactions of all four antibodies with  $\text{A}\beta(1-40)$  are characterized by a 1mAb:2 $\text{A}\beta$  stoichiometry. All binding affinities fall in the narrow range of  $\Delta G_{\text{A}\beta}^0 = -10.8$  to  $-9.8$  kcal/mol (at 28  $^\circ\text{C}$ ) and are summarized in Table 1. Moreover, the binding is an enthalpy-driven process with favorable negative enthalpy changes and unfavorable binding entropies. The only exception is antibody B24-C40, which exhibits a small positive entropy change. Inspection of Table 1 also demonstrates that the measured enthalpies  $\Delta H_{\text{A}\beta}^0$  vary considerably between  $-8.1$  and  $-19.4$  kcal/mol. On the other hand, as the free energy  $\Delta G_{\text{A}\beta}^0$  remains fairly constant, a linear relationship between the enthalpy,  $\Delta H_{\text{A}\beta}^0$ , and the entropy term,  $T\Delta S_{\text{A}\beta}^0$ , can be predicted and is experimentally verified in Figure 2. Here the reaction enthalpy,  $\Delta H_{\text{A}\beta}^0$ , is plotted vs the entropy term  $T\Delta S_{\text{A}\beta}^0$  and yields a straight line with a slope close to unity.

In many protein-protein interactions the reaction enthalpy is affected by a change in temperature. To determine the heat capacity change associated with the antibody- $\text{A}\beta$  binding reaction, ITC experiments for all four antibodies were performed in the range of 15 to 40  $^\circ\text{C}$ . The results obtained for B24-C40 are shown in Figure 3. The upper panel displays the variation of  $\Delta H_{\text{A}\beta}^0$  with temperature. From the slope of the straight line the change in the heat capacity referenced to  $\text{A}\beta$  binding can be determined as  $\Delta C_{p,\text{A}\beta}^0 = -361$  cal/(mol K). The  $\Delta C_{p,\text{A}\beta}^0$  values of the other three antibodies are also negative, but smaller in magnitude by about a factor of  $\sim 2$  (cf. Table 1).

The bottom panel in Figure 3 displays the variation of the dissociation constant with temperature. The solid line corresponds to the prediction based on the integration of the van't Hoff equation,  $\partial \ln K/\partial T = \Delta H/RT^2$ , using the experimentally derived temperature-dependent enthalpy. As expected for an exothermic reaction, the dissociation constant increases with increasing temperature.

The large heat capacity change then provides an explanation for the enthalpy-entropy compensation phenomenon, that is,

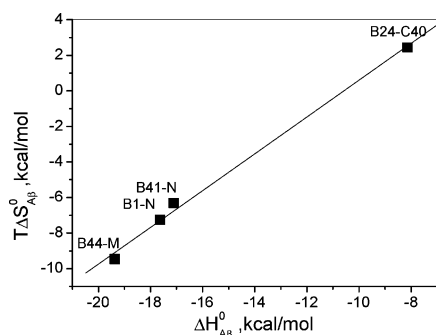


**Figure 2.** Enthalpy–entropy compensation plot for the antibody–A $\beta$  binding reaction. Comparison of four different antibodies. ITC measurements were performed in 25 mM HEPES buffer at pH 7.4 and 28 °C.

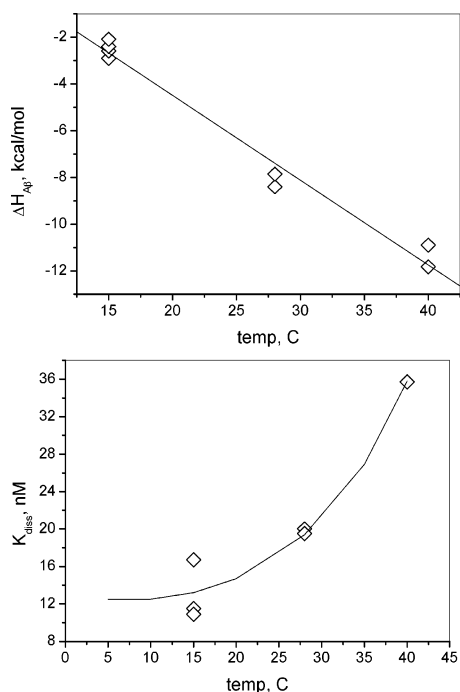


**Figure 3.** Temperature dependence of the thermodynamic binding parameters for the binding of antibody B24-C40 to A $\beta$ (1–40) in buffer (25 mM HEPES, pH 7.4). Upper panel: Variation of  $\Delta H_{A\beta}^0$  with temperature. The regression line corresponds to  $\Delta H_{A\beta}^0(T)$  (kcal/mol) =  $-0.363T + 2.77$ . Lower panel: Variation of the dissociation constant,  $K_{diss}$ , with temperature. The solid line is the theoretical prediction based on the van't Hoff equation calculated with a temperature-dependent  $\Delta H_{A\beta}^0$ .

the linear correlation between  $\Delta H_{A\beta}^0$  and  $T\Delta S_{A\beta}^0$ . The temperature coefficient of  $\Delta H_{A\beta}^0$  is  $\Delta C_p^0$ , and that of  $T\Delta S_{A\beta}^0$  is  $C_p^0 + \Delta S_{A\beta}^0$ . As  $C_p^0 \gg \Delta S_{A\beta}^0$  (cf. Table 1) the two thermodynamic parameters  $\Delta H_{A\beta}^0$  and  $T\Delta S_{A\beta}^0$  vary in parallel (within the accuracy of the present ITC measurements).

## Discussion

Isothermal titration calorimetry was used to determine the thermodynamic parameters of the equilibrium between different antibodies and essentially monomeric, soluble A $\beta$ (1–40). The binding stoichiometry for IgG antibodies is 1mAb:2A $\beta$ . The binding constants vary by about a factor of 4 and fall in the range of  $7.2 \times 10^7 \text{ M}^{-1}$  for B41-N to  $1.6 \times 10^7 \text{ M}^{-1}$  for B44-M (at 28 °C).

The corresponding free energies are  $\Delta G_{A\beta}^0 = -10.8$  to  $-9.9$  kcal/mol. On the basis of 26 examples, the average  $\Delta G^0$  for

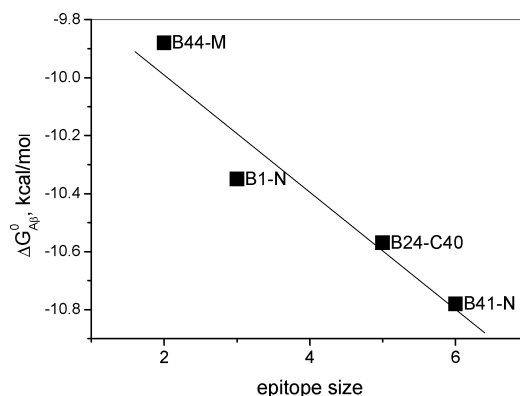


**Figure 4.** Free energy of binding,  $\Delta G_{A\beta}^0$ , as a function of the number of amino acids,  $k$ , constituting the epitope recognized by the different antibodies. The regression line corresponds to  $\Delta G_{A\beta}^0$  (kcal/mol) =  $-0.202k - 9.587$ .

protein–peptide interaction has been reported as  $-8.5 \pm 1.88$  kcal/mol corresponding to an average binding constant of  $1.8 \times 10^6 \text{ M}^{-1}$ .<sup>20</sup> The antibody–A $\beta$  binding energies are at the upper boundary of this average value and the binding constants of A $\beta$  to the different antibodies are hence larger by about a factor of 10–20 than for other protein–peptide interactions.

The binding of the antibodies was also measured with surface plasmon resonance (SPR) under equilibrium conditions. The stoichiometry of the reaction cannot be determined by this method. Table 1 includes dissociation constants measured with ITC and surface plasmon resonance agree within a factor of 1.5 for B1-N and B44-M. Larger discrepancies are, however, observed for the two other antibodies studied. Similar differences between ITC and SPR have also been observed for other systems.<sup>21–23</sup> In the present study this may reflect the different behavior of antibodies when binding to antigens on a solid support compared to antigens in solution. Curved Scatchard plots were observed for antibodies B24-C40 and B41-N, which indicates that bivalent binding of the antibodies could not be fully suppressed even though the density of the immobilized A $\beta$  peptide was reduced as much as possible.

All four antibody–A $\beta$  reactions are characterized by a large negative change in heat capacity. According to the hydrophobic effect a negative  $\Delta C_p$  arises from the release of hydration water if nonpolar, solvent-accessible surface areas meet to form a purely hydrophobic complex. However, release of hydration water should also make a substantial positive entropy contribution. This is contradicted by the unfavorable entropy changes observed in the present antibody–A $\beta$  interaction. Similar observations have been made for other systems and it is thus unlikely that the hydrophobic effect is the only driving force for complex formation. For example, a detailed thermodynamic study has been provided for the complex formed between the Fv fragment of the anti-hen egg white lysozyme (HEL) antibody D1.3 and HEL.<sup>24</sup> D1.3–HEL complex formation is largely dependent on a functional epitope composed of three amino acids. The binding constant is  $5 \times 10^7 \text{ M}^{-1}$ , the reaction enthalpy  $\Delta H^0 = -21.5$  kcal/mol, and the entropy term  $T\Delta S^0 = -11.0$  kcal/mol. These numbers are comparable to those obtained for the mAb:A $\beta$  complex formation (cf. Table 1). On the basis of the crystal structures of the reactants and that of the D1.3–HEL complex the authors conclude that the change in the hydrophobic area makes a small positive contribution to the reaction entropy which is, however, overcompensated by a larger negative entropy that is interpreted as a loss in confor-



mational freedom. No heat capacity measurements were made for this system.

Qualitatively and quantitatively similar results were also obtained for the interaction of the complement component C3 with its inhibitor compstatin.<sup>23</sup> The complex formation is enthalpy driven with a large negative heat capacity change  $\Delta C_p$ , while the reaction entropy is negative. Again water release appears to be more than compensated by a conformational stiffening of the complex.

The antibodies employed in this study recognize different epitopes of the peptides  $A\beta(1-40)$  and  $A\beta(1-42)$ . B1-N and B41-N are specific for the polar N-terminal region, whereas B44-M detects the middle region of  $A\beta$  with two vicinal Phe residues that are believed to be important for the formation of the secondary structure. Finally, B24-C40 recognizes the C-terminal amino acids of  $A\beta(1-40)$  (but not  $A\beta(1-42)$ ) which are part of the hydrophobic transmembrane region of the amyloid precursor protein APP. No high-resolution structure of  $\beta$ -amyloid fibrils exists but the available X-ray and NMR data converge on a model in which the first 10 residues of  $A\beta(1-40)$  are structurally disordered in fibrils while residues 12–24 and 30–40 adopt  $\beta$ -strand conformations and form parallel  $\beta$ -sheets through intermolecular hydrogen bonding.<sup>25</sup> In terms of this model, antibodies B1-N and B41-N are directed against the flexible region, B24-C40 and B44-M against the more rigid cross- $\beta$  structural motif. It should be noted, however, that in dilute  $A\beta(1-40)$  solutions such as used in the ITC experiment, the CD spectra reveal an essentially random-coil structure of  $A\beta(1-40)$ .<sup>7</sup> The  $\beta$ -strand conformation will therefore be formed only upon interaction with the antibody. The binding of  $A\beta(1-40)$  is thus a two-state reaction in which ligand binding is coupled to a conformational transition, a process similar to that of other protein–ligand interactions.<sup>26</sup> Unfortunately, it is not possible to derive independent information on the folding dynamics from CD spectroscopy as the CD spectrum is dominated by the antibody contribution. It is clear, however, that the random coil  $\rightarrow$   $\beta$ -structure transition will make a negative contribution to the reaction entropy.

Among the four antibodies tested, B41-N has the highest affinity for  $A\beta(1-40)$  with a dissociation constant of  $\sim 14$  nM. The specificity for the N-terminal domain was confirmed by additional ITC measurements where  $A\beta(1-40)$  was replaced by an  $A\beta(1-40)$  analogue in which amino acids 5 and 6 were substituted with their D-enantiomers. No binding could be detected with ITC.

Compared to the variations in  $\Delta H_{A\beta}^0$  and  $\Delta S_{A\beta}^0$  of the four antibodies, the free energy  $\Delta G_{A\beta}^0$  remains fairly constant for all four antibodies. Nevertheless, we observe some systematic change with the size of the epitope. Figure 4 shows a plot of the change in free energy vs the number of amino acids,  $k$ , of the epitope recognized. The approximately linear dependence is characterized by the regression line  $\Delta G_{A\beta}^0$  (kcal/mol) =  $-0.202k - 9.587$ . Each additional amino acid in the epitope would increase the association constant by a factor of about 1.4. For an epitope of the size of ten amino acids the dissociation constant can be expected to be at least by an order of magnitude smaller than that of a two amino acid epitope.

B24-C40 has only the second largest epitope (5aa) measured in this series but exhibits by far the largest heat capacity change,  $\Delta C_{p,A\beta}$ , which exceeds those of the other antibodies by a factor of 2. As B24-C40 is directed against the hydrophobic C-terminal region of  $A\beta$  it could be speculated that the large negative  $C_p$  is caused by a particularly large hydrophobic area buried in the mAb– $A\beta$  complex. In protein *folding* studies, such a correlation

was indeed found between the value of  $\Delta C_p$  and the amount of hydrophobic surface buried.<sup>27–29</sup> On the other hand, it has been pointed out that such a correlation may not exist for *protein–protein interactions*.<sup>20</sup> In fact, the removal of large hydrophobic residues buried in the interface may even result in  $\Delta C_p$  values more *negative* compared to those of the unmodified protein. Without a detailed knowledge of the molecular structure of the antibody– $A\beta$  complex a molecular interpretation of the  $\Delta C_p$  value is therefore not possible. More insight could be expected from studies with additional antibodies against the C-terminal  $A\beta(1-42)$  peptide. Because  $A\beta(1-42)$  has the strong tendency to aggregate and to precipitate from solution, ITC studies will be experimentally more demanding than the present one.

As  $A\beta$  peptides exhibit a low solubility, fibril formation is often considered to be an irreversible process with low dissociation rates. However, formation of fibrils from  $A\beta(1-40)$  is a true dynamic equilibrium, in which fibrils are in equilibrium with a characteristic monomer concentration.<sup>11</sup> In addition, solution conditions have been identified under which two types of soluble oligomers of  $A\beta(1-40)$  could be trapped and stabilized for an extended period of time.<sup>30</sup> Since monomers, oligomers, and fibrils appear to be in equilibrium, removal of monomers by binding to antibodies may eventually lead to a dissolution of fibrils and oligomers.

Our study is limited to freshly prepared solutions of  $A\beta(1-40)$  containing few if any amyloid aggregates. Therefore, we cannot assess the antibody interaction with soluble  $A\beta$  oligomers which are considered to be the main pathological species of amyloid.<sup>31</sup> However, since monomers and oligomers are in equilibrium we do not expect a major influence of the thermodynamic parameters if the antibodies recognize only monomeric  $A\beta$ . From the point of therapeutic utility a selectivity for monomers could be an advantage since the antibody will remove the monomers from the equilibrium.<sup>5,32</sup> On the other hand, polyclonal antibodies have been described which detect soluble  $A\beta(1-40)$  oligomers, but not fibrils or monomers. Surprisingly, these antibodies are not sequence-specific but react with a wide variety of amyloidogenic proteins and peptides.<sup>33</sup>

In summary, the present study provides the first thermodynamic analysis of an antibody– $A\beta(1-40)$  complex formation. Each antibody binds 2  $A\beta$  and the binding constants are in the range of  $10^7$ – $10^8$  M<sup>−1</sup> and comparable to those of other antibody–antigen complex formations. The binding reaction is driven by enthalpy but counteracted by a negative entropy change. The hydrophobic effect appears to make only a small contribution to mAb: $A\beta$  complex formation.

**Acknowledgment.** This work was supported by Grant No. 3100-107793 of the Swiss National Science Foundation.

## References and Notes

- (1) Schenk, D.; Barbour, R.; Dunn, W.; Gordon, G.; Grajeda, H.; Guido, T.; Hu, K.; Huang, J.; Johnson-Wood, K.; Khan, K.; Kholodenko, D.; Lee, M.; Liao, Z.; Lieberburg, I.; Motter, R.; Mutter, L.; Soriano, F.; Shopp, G.; Vasquez, N.; Vandeventer, C.; Walker, S.; Wogulis, M.; Yednock, T.; Games, D.; Seubert, P. *Nature* **1999**, *400*, 173.
- (2) Nicoll, J. A.; Wilkinson, D.; Holmes, C.; Steart, P.; Markham, H.; Weller, R. O. *Nat. Med.* **2003**, *9*, 448.
- (3) Bard, F.; Barbour, R.; Cannon, C.; Carretto, R.; Fox, M.; Games, D.; Guido, T.; Hoenow, K.; Hu, K.; Johnson-Wood, K.; Khan, K.; Kholodenko, D.; Lee, C.; Lee, M.; Motter, R.; Nguyen, M.; Reed, A.; Schenk, D.; Tang, P.; Vasquez, N.; Seubert, P.; Yednock, T. *Proc. Natl. Acad. Sci. U.S.A.* **2003**, *100*, 2023.
- (4) McLaurin, J.; Cecal, R.; Kierstead, M. E.; Tian, X.; Phinney, A. L.; Manea, M.; French, J. E.; Lambermon, M. H. L.; Darabie, A. A.; Brown, M. E.; Janus, C.; Chishtii, M. A.; Horne, P.; Westaway, D.; Fraser, P. E.; Mount, H. T. J.; Przybylski, M.; St. George-Hyslop, P. *Nat. Med.* **2002**, *8*, 1263.

- (5) DeMattos, R. B.; Bales, K. R.; Cummins, D. J.; Dodart, J. C.; Paul, S. M.; Holtzman, D. M. *Proc. Natl. Acad. Sci. U.S.A.* **2001**, *98*, 8850.
- (6) Bokvist, M.; Lindstrom, F.; Watts, A.; Grobner, G. *J. Mol. Biol.* **2004**, *335*, 1039.
- (7) Terzi, E.; Holzemann, G.; Seelig, J. *J. Mol. Biol.* **1995**, *252*, 633.
- (8) Terzi, E.; Holzemann, G.; Seelig, J. *Biochemistry* **1997**, *36*, 14845.
- (9) Janek, K.; Rothmund, S.; Gast, K.; Beyermann, M.; Zipper, J.; Fabian, H.; Bienert, M.; Krause, E. *Biochemistry* **2001**, *40*, 5457.
- (10) Harper, J. D.; Lansbury, P. T., Jr. *Annu. Rev. Biochem.* **1997**, *66*, 385.
- (11) Williams, A. D.; Shivaprasad, S.; Wetzal, R. *J. Mol. Biol.* **2006**, *357*, 1283.
- (12) Hortschansky, P.; Schroeckh, V.; Christopeit, T.; Zandomeneghi, G.; Fandrich, M. *Protein Sci.* **2005**, *14*, 1753.
- (13) Hortschansky, P.; Christopeit, T.; Schroeckh, V.; Fandrich, M. *Protein Sci.* **2005**, *14*, 2915.
- (14) Sengupta, P.; Garai, K.; Sahoo, B.; Shi, Y.; Callaway, D. J.; Maiti, S. *Biochemistry* **2003**, *42*, 10506.
- (15) Gorman, P. M.; Yip, C. M.; Fraser, P. E.; Chakrabarty, A. *J. Mol. Biol.* **2003**, *325*, 743.
- (16) Wiseman, T.; Williston, S.; Brandts, J. F.; Lin, L. N. *Anal. Biochem.* **1989**, *179*, 131.
- (17) Ababou, A.; Ladbury, J. E. *J. Mol. Recognit.* **2006**, *19*, 79.
- (18) van Holde, K. E.; Johnson, W. C.; Ho, P. S. Chemical equilibria involving Macromolecules. In *Principles of Physical Chemistry*; Challice, J., Ed.; Prentice Hall: Upper Saddle River, NJ, 1998; p 604.
- (19) Hammes, G. G. Ligand binding to macromolecules. In *Thermodynamics and kinetics for the biological sciences*; Wiley-Interscience: New York, 2000; p 124.
- (20) Stites, W. E. *Chem. Rev.* **1997**, *97*, 1233.
- (21) Fanghänel, J.; Fischer, G. *Biophys. Chem.* **2003**, *100*, 351.
- (22) Hernaiz, M. J.; LeBrun, L. A.; Wu, Y.; Sen, J. W.; Linhardt, R. J.; Heegaard, N. H. *Eur. J. Biochem.* **2002**, *269*, 2860.
- (23) Katragadda, M.; Morikis, D.; Lambris, J. D. *J. Biol. Chem.* **2004**, *279*, 54987.
- (24) Sundberg, E. J.; Urrutia, M.; Braden, B. C.; Isern, J.; Tsuchiya, D.; Fields, B. A.; Malchiodi, E. L.; Tormo, J.; Schwarz, F. P.; Mariuzza, R. A. *Biochemistry* **2000**, *39*, 15375.
- (25) Petkova, A. T.; Ishii, Y.; Balbach, J. J.; Antzutkin, O. N.; Leapman, R. D.; Delaglio, F.; Tycko, R. *Proc. Natl. Acad. Sci. U.S.A.* **2002**, *99*, 16742.
- (26) Cliff, M. J.; Williams, M. A.; Brooke-Smith, J.; Barford, D.; Ladbury, J. E. *J. Mol. Biol.* **2005**, *346*, 717.
- (27) Privalov, P. L.; Gill, S. J. *Adv. Protein Chem.* **1988**, *39*, 191.
- (28) Murphy, K. P.; Freire, E. *Adv. Protein Chem.* **1992**, *43*, 313.
- (29) Spolar, R. S.; Record, M. T., Jr. *Science* **1994**, *263*, 777.
- (30) Huang, T. H.; Yang, D. S.; Plaskos, N. P.; Go, S.; Yip, C. M.; Fraser, P. E.; Chakrabarty, A. *J. Mol. Biol.* **2000**, *297*, 73.
- (31) Walsh, D. M.; Klyubin, I.; Fadeeva, J. V.; Cullen, W. K.; Anwyl, R.; Wolfe, M. S.; Rowan, M. J.; Selkoe, D. J. *Nature* **2002**, *416*, 535.
- (32) Dodart, J. C.; Bales, K. R.; Gannon, K. S.; Greene, S. J.; DeMattos, R. B.; Mathis, C.; DeLong, C. A.; Wu, S.; Wu, X.; Holtzman, D. M.; Paul, S. M. *Nat. Neurosci.* **2002**, *5*, 452.
- (33) Kaye, R.; Head, E.; Thompson, J. L.; McIntire, T. M.; Milton, S. C.; Cotman, C. W.; Glabe, C. G. *Science* **2003**, *300*, 486.